J Mater Sci (2009) 44:2143–2151
DOI 10.1007/s10853-009-3295-0

Studies of surface-modified wood flour/polypropylene composites

**Yongcheng Zhang · Hossein Toghiani ·
Jilei Zhang · Yibin Xue · Charles U. Pittman Jr.**

Received: 29 October 2008 / Accepted: 22 January 2009 / Published online: 26 February 2009

Abstract Wood flour (WF)/polypropylene (PP) composites have been made by extrusion and hot press compression molding. The composite water uptake and flexural properties were investigated. The composite fracture surfaces were studied by SEM. WF esterified with octanoyl chloride was used in WF/PP composites to improve the composites' water resistance. Maleated polypropylene (MAPP) was also studied and compared with esterification by acid chlorides. Esterification by octanoyl chloride reduced the composite water uptake. However, the C_8 chain is still not long enough to form effective entanglements with the PP matrix. So, despite enhancements in hydrophobic interactions, flexural strengths and flexural moduli decreased. MAPP (MW = 47000) polymer chains can entangle with the matrix polypropylene molecules. Therefore, when MAPP's maleic anhydride functions esterify WF surface hydroxyls, improved water resistance and composite flexural properties were achieved. The modifier chain length is of critical importance and more important than the surface density of hydrophobic groups for improving WF–PP interfacial adhesion and composite mechanical performance.

Introduction

High oil prices have induced a change in consumption habits. Renewable and low energy-cost materials are gaining popularity. The use of light weight, renewable natural materials instead of heavy metal or mineral-based materials is important to generate lighter materials. Wood flour (WF) has advantages, including low density, renewability, and availability [1]. It has been used as a filler in polymeric composites [1]. WF/PP composites have the largest market share among natural fiber/plastic composites in building materials, furniture, and internal car parts [1–3]. Addition of WF improves PP composite stiffness. WF/PP composites have acceptable mechanical properties, but surface incompatibility between WF and PP, and water absorption by WF/PP composites are still major problems. They cause degradation and mechanical performance losses [4–8]. These problems are caused by the hydrophilic hydroxyl groups existing in the WF's structures.

The WF/PP composite properties can be improved by modifications of the WF and the PP matrix. The choice of modifiers is critical to composite performance. Maleated polypropylene (MAPP) is the most researched additive to improve the WF–PP compatibility and adhesive bonding at the interface [9–11], although other methods have been

---

Y. Zhang · C. U. Pittman Jr. (✉)
Department of Chemistry, Mississippi State University,
Mississippi State, MS 39762, USA
e-mail: CPittman@chemistry.msstate.edu;
cpittman@ra.msstate.edu

H. Toghiani
Dave C. Swalm School of Chemical Engineering, Mississippi
State University, Mississippi State, MS 39762, USA

J. Zhang
Department of Forest Products, Mississippi State University,
Mississippi State, MS 39762, USA

Y. Xue
Center for Advanced Vehicular Systems, Mississippi State
University, Mississippi State, MS 39762, USA

Present Address:
Y. Xue
Department of Mechanical and Aerospace Engineering,
Utah State University, Logan, UT 84322-4100, USA

investigated [6, 12]. We previously converted WF surface OH groups to hydrophobic ester groups, greatly reducing water uptake [13]. When appropriately modified, WF reinforcement can improve composite stiffness and strength.

In this research, WF was esterified by octanoyl chloride in either chloroform or dimethylformide. Octanoyl chloride is a small molecule acid chloride which can be reacted in high yields with a high density of surface hydroxyl groups by esterification. MAPP is a large polymer molecule that can only form a low density of ester bonds to surfaces. The effects of octanoyl chloride esterification of WF versus MAPP addition to the PP matrix (and esterification of WF surfaces) on the composites' water absorption and mechanical properties were investigated in order to compare these two approaches. These results were compared to those of unmodified WF/PP composites prepared identically.

The smaller octanoyl chloride should be able to esterify a higher fraction of surface region hydroxyl groups while forming a hydrophobic WF surface. In contrast, a smaller fraction of surface hydroxyl groups will react with MAPP since diffusion of the large polymeric MAPP is sterically blocked by the larger surface region coverage of each MAPP molecule and slower MAPP diffusion rates. MAPP chains can better entangle with the PP matrix and each MAPP at the WF surface may have a larger effect on enhancing surface hydrophobicity than a single C-8 ester function. Nevertheless, surface hydroxyl functions will remain unesterified in the vicinity of each surface-bound MAPP. Therefore, comparing octanoyl chlorides versus MAPP modifications is of interest.

All the composites were prepared by melt blending in an extruder and hot press compression molding. The composite flexural strengths and flexural moduli were obtained by third-point bending tests. Fracture surfaces were investigated by SEM.

Experimental

Materials

Southern pine wood flour (80 mesh, 180 μm) was provided by American Wood Fibers Inc. PP (AP 7710, melt flow rate = 10 g/10 min at 190 °C/2.16 kg) was provided by Huntsman Corporation. The PP melting temperature range was 169–182 °C. PP was ground into a powder (<2 mm) before use. Maleated polypropylene, MAPP, (G-3015, MW = 47000, maleic anhydride <1.0 wt%) was provided by Eastman Chemical Company. WF was esterified with octanoyl chloride in chloroform and in DMF as described in our previous study [13]. *p*-Dimethylaminopyridine was used to catalyze these esterifications and triethylamine was the stoichiometric base [13].

Preparation of composite blends by extrusion

The composite components were premixed with a Teledyne Readco mixer (York, PA, USA) at room temperature. Then the mixtures were further melt-blended by a high shear, single screw microextruder (Model: RCPR-0625 Compounder from Randcastle Extrusion Systems, Inc.). A screw rotation speed of 35 rpm was used. All the five heating zones of the extruder were set at 182 °C. The extruded samples were cooled to room temperature and then granulated into small pieces (<4 mm) using a Model 4 Laboratory Mill (Arthur H. Thomas Company).

Three levels of WF were investigated. WF/PP weight ratios of 20/100, 40/100, and 60/100 were employed. WF that was unmodified was used at all these levels. Esterified WF and WF with added MAPP were then compared at these same WF/PP ratios.

Preparation of composite panels by compression molding

A PHI Q-23 compression hot press (Tulip Corporation) was preheated to 182 °C. A specified amount of the granulated WF/PP blend was weighed into a mold (127 mm length × 76.2 mm width). The mold was placed on the press for about 20 min and the PP melted. Then the pressure was raised to 1.8 MPa and this pressure was maintained for 20 min. Subsequently, the pressure was raised to 3.6 MPa and then the heating elements were turned off. When the temperature dropped to 32–37 °C, the pressure was released and the sample was removed. Sample panels were cut for water absorption and mechanical tests.

Third-point bending tests

Five specimens were tested in bending according to ASTM standard D790-92 [14] for each treatment group (C_8-WF and MAPP-PP), both before and after water absorption testing. The specimen size was 76.2 mm × 25.4 mm × 3.2 mm. All the specimens were tested on an Instron 5869 testing machine with a crosshead speed of 1.27 mm/min.

Water absorption tests

Water absorption tests were conducted according to ASTM standard D570-98 [15]. The specimens were entirely immersed in distilled water for 24 h. The percentage increase in weight during immersion was calculated. Five

76.2 mm × 25.4 mm × 3.2 mm specimens were tested for each treatment group.

SEM of WF/PP composite fracture surfaces

SEM was performed using a JEOL JSM-6500F 5.0 kV scanning electron microscope. The sample surfaces to be observed were coated with a thin layer of Pd/Au (~7 nm) before testing.

Results and discussion

Unmodified-WF/PP composites with different WF loadings

The properties of unmodified-WF/PP composites are highly dependent on the WF loading (Fig. 1). High WF weight fractions increase the composite hardness, but they may also decrease the composite strength due to the defects existing in the WF/PP interfaces. The hydrophilic WF's surface area and the total amount of –OH increase as the WF content increases. Both of these features increase the rate and amount of water uptake. Furthermore, the WF can eventually absorb water throughout fiber particles.

Unmodified-WF/PP 20/100, 40/100, and 60/100 (w/w) composites were prepared. This series of unmodified-WF/PP composites were designed to investigate the effect of unmodified-WF loading on composite water absorption and mechanical properties.

Water absorption tests

The water absorbed by unmodified-WF/PP composites at different WF loadings are summarized in Fig. 1. The amount of water absorbed by the composites increased significantly when the water immersion time changed from 2 to 24 h (Fig. 1). The difference in water absorption after 2 h among the 20/100, 40/100, and 60/100 (w/w) WF/PP composites was small, because only a small amount of water absorption had occurred at this stage and the systems were far from equilibrium. Composites with higher unmodified-WF loadings absorbed significantly greater amounts of water at 24 h (Fig. 1). The 24-h water absorption of unmodified-WF/PP (60/100) was more than four times that of unmodified-WF/PP (20/100) composites. It is obvious that the water absorption is highly dependent on the WF loading. Water absorption studies showed that uptake continued and even after a one-week period, equilibrium had still not been achieved. These data are not included.

Third-point bending tests

Third-point bending tests were conducted to obtain the composite flexural strengths and flexural moduli. Figures 2 and 3 summarize the flexural strengths and flexural moduli of (20/100), (40/100), and (60/100) WF/PP composites before and after water immersion for 24 h, respectively.

The composite flexural strength decreased only slightly with an increase in WF loading in the composites, both before and after water immersion (24 h) (Fig. 2). This

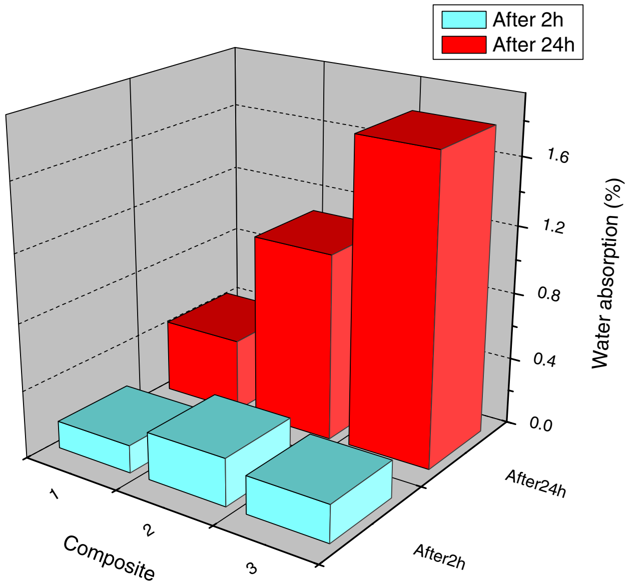

Fig. 1 Water absorption of unmodified-WF/PP composites with different WF loadings. Composite 1: WF/PP (20/100); composite 2: WF/PP (40/100); composite 3: WF/PP (60/100)

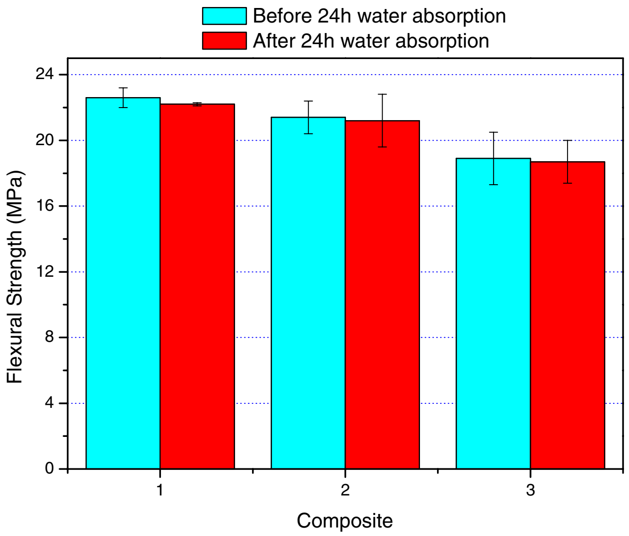

Fig. 2 Flexural strengths of unmodified-WF/PP composites with different WF loadings before and after a 24-h water immersion. Composite 1: WF/PP (20/100); composite 2: WF/PP (40/100); composite 3: WF/PP (60/100)

decrease is most pronounced at 60/100 WF/PP ratios. WF/PP composite flexural strengths remained almost constant after a 24-h immersion in water.

The composite flexural moduli increased substantially (in contrast to strengths) with WF loading (Fig. 3). The flexural moduli decreased at each WF loading after the 24-h water immersion and this decrease was most pronounced at the largest WF loading. The water absorption occurs within the WF portion of unmodified-WF/PP composites. Water absorption can modify wood fiber mechanical properties and induce dimensional changes by swelling individual fibers. Water moving into the cell walls increases cellulose and hemicellulose hydration. This could cause the decrease in unmodified-WF/PP composite moduli. Other long-term problems include fungal and bacterial growth which would eventually degrade unmodified-WF if sufficient moisture is present.

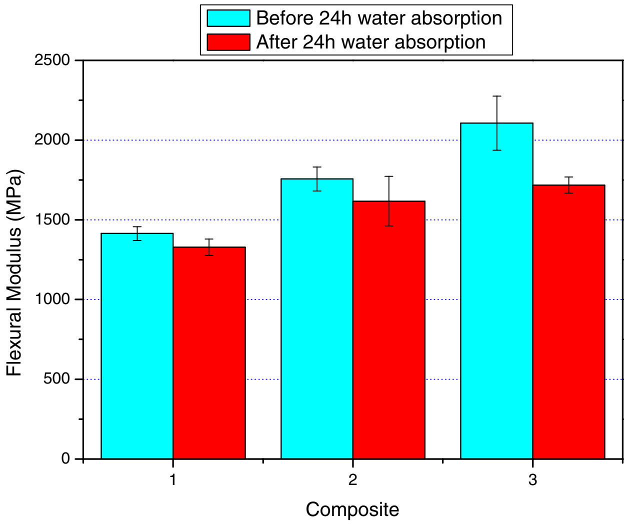

Fig. 3 Flexural moduli of unmodified-WF/PP composites with different WF loadings before and after a 24-h water immersion. Composite 1: WF/PP (20/100); composite 2: WF/PP (40/100); composite 3: WF/PP (60/100)

SEM of unmodified-WF/PP composite fracture surfaces

SEM of fracture surfaces were obtained to investigate the unmodified-WF dispersion in the PP matrix and the nature of unmodified-WF–PP interface. Fracture surfaces are shown of unmodified-WF/PP (20/100) composites (Fig. 4a, b) and (60/100) composites (Fig. 4c, d). No obvious differences in WF dispersion and WF–PP bonding were observed between these WF loadings. Unmodified-WF was well dispersed in the PP matrix (Fig. 4a, c). Many fibers were exposed in the fracture surface (Fig. 4a, c) with little or no PP adhering to the fiber surfaces. This is most easily observed in the higher magnifications (Fig. 4b, d, see arrows). This shows that facture failure mainly occurred at the unmodified-WF–PP interface instead of within the PP matrix. This demonstrates that the WF–PP matrix bonding was weak. The difference in mechanical properties

Fig. 4 SEM micrographs of unmodified-WF/PP composites with different WF loadings: **a**, **b** WF/PP (20/100); **c**, **d** WF/PP (60/100)

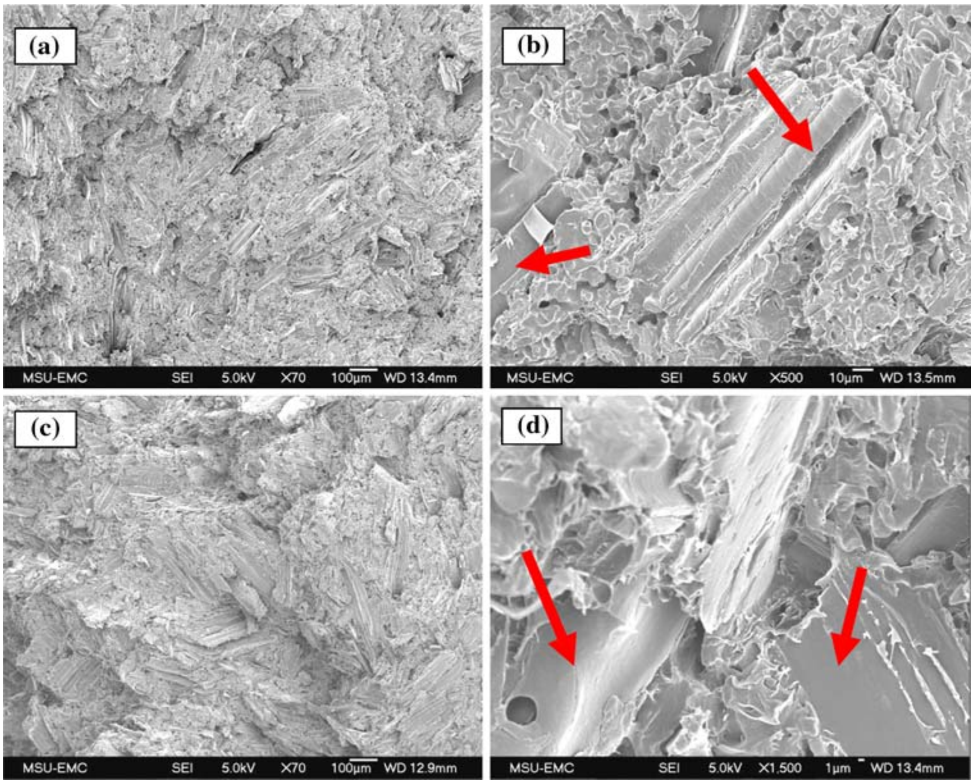

between the (20/100) and (60/100) composites was mainly attributed to the change in WF content, but not to the differences in WF–PP bonding or WF dispersion.

Effects of WF esterification and use of modification effects

Two types of modified WF, namely, C_8-WF($CHCl_3$) (WF esterified with octanoyl chloride in the solvent, chloroform, weight gain +10%) and C_8-WF(DMF) (WF esterified with octanoyl chloride in dimethylformamide (DMF), weight gain +80%), were prepared [13] and then used in the C_8-esterified WF/PP composites. C_8-WF($CHCl_3$)/PP (60/100) and C_8-WF(DMF)/PP (60/100) composites were prepared. The weight of WF instead of the weight of the esterified WF was used in the composite formulations. This kept the amount of fiber reinforcement the same for comparison with composites made with unmodified WF. For example, in the C_8-WF($CHCl_3$)/PP (60/100) composite, the 60 represents the weight of WF, not the weight of C_8-WF($CHCl_3$). The real weight of this C_8-WF($CHCl_3$) was $60 + 60 \times 0.1 = 66$. Unmodified-WF/PP/MAPP composites with different MAPP concentrations (1, 2, and 5 percent the weight of PP) were also prepared. Both of these types of composites were compared to the unmodified-WF/PP composites.

Water absorption tests

Figure 5 shows the water absorbed by unmodified WF/PP, C_8-WF/PP composites, and unmodified-WF/PP/MAPP composites with WF/PP = 60/100. After a 2-h immersion in water, the weight gains of unmodified-WF/PP, C_8-WF/PP, and unmodified-WF/MAPP/PP composites were <0.3%. However, the extent of water absorption by these composites increased as immersion time increased to 24 h. Water uptake was much greater for the unmodified-WF/PP composites (composite 1) than for the C_8-WF/PP composites (composites 5–6), and composites containing MAPP (composites 2–4). MAPP addition reduced the 24-h water absorption weight gain of unmodified-WF/PP composites. The higher the MAPP loading, the lower the 24-h water absorption weight gain became (composites 2–4). The C_8-WF(DMF)/PP (60/100) composite absorbed far less water in 24 h (0.324%, composite 5) than any of the other composites. C_8-esterified or employing MAPP are effective at decreasing the rate of water uptake.

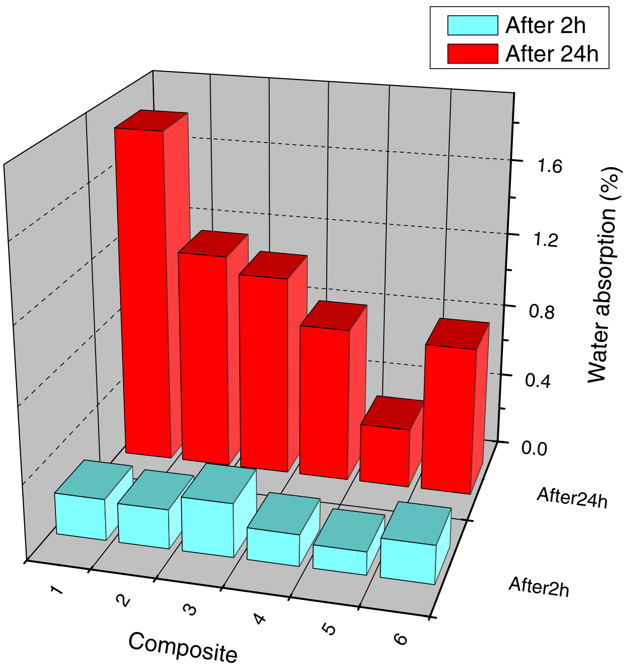

Fig. 5 Water-absorption weight gain of unmodified-WF/PP, C_8-WF/PP, and unmodified-WF/MAPP/PP composites. Composite 1: WF/PP (60/100); composite 2: WF/MAPP/PP (60/1/100); composite 3: WF/MAPP/PP (60/2/100); composite 4: WF/MAPP/PP (60/5/100); composite 5: C_8-WF(DMF)/PP (60/100); composite 6: C_8-WF($CHCl_3$)/PP (60/100)

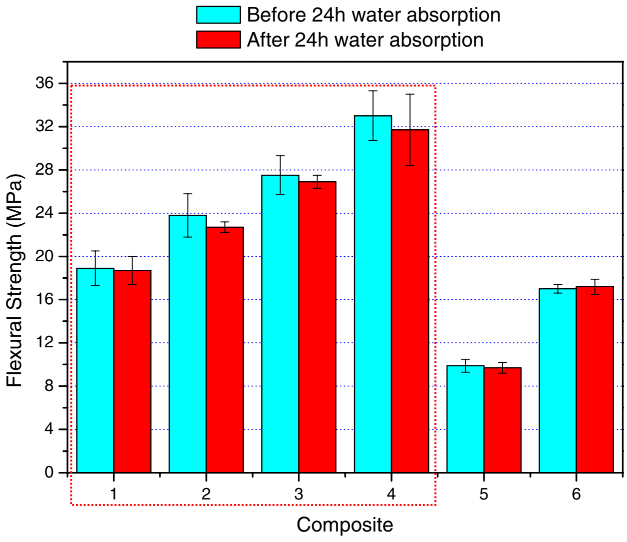

Fig. 6 Flexural strengths of unmodified-WF/PP, C_8-WF/PP, and unmodified-WF/MAPP/PP composites before and after 24-h immersion in water. Composite 1: WF/PP (60/100); composite 2: WF/MAPP/PP (60/1/100); composite 3: WF/MAPP/PP (60/2/100); composite 4: WF/MAPP/PP (60/5/100); composite 5: C_8-WF(DMF)/PP (60/100); composite 6: C_8-WF($CHCl_3$)/PP (60/100)

Third-point bending tests

The flexural strengths of unmodified-WF/PP, C_8-WF/PP, and unmodified-WF/MAPP/PP composites with WF/PP = 60/100 (before and after 24 h of water immersion) are illustrated in Fig. 6. The flexural moduli of these same composites (before and after 24 h of water immersion) are illustrated in Fig. 7.

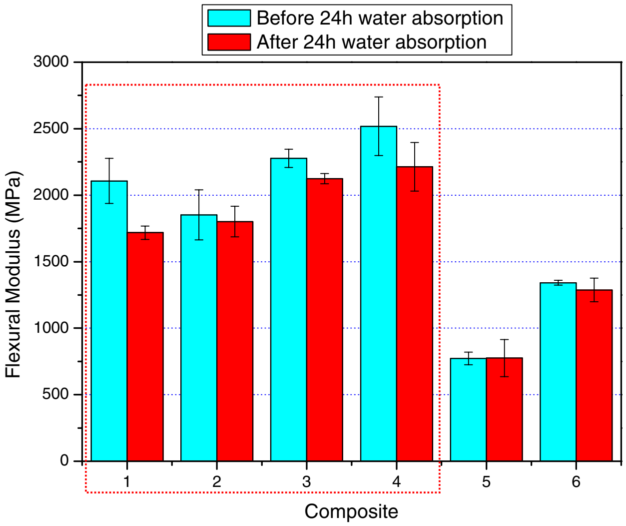

Fig. 7 Flexural moduli of unmodified-WF/PP, C_8-WF/PP, and unmodified-WF/MAPP/PP composites before and after 24-h water immersion. Composite 1: WF/PP (60/100); composite 2: WF/MAPP/PP (60/1/100); composite 3: WF/MAPP/PP (60/2/100); composite 4: WF/MAPP/PP (60/5/100); composite 5: C_8-WF(DMF)/PP (60/100); composite 6: C_8-WF(CHCl$_3$)/PP (60/100)

The composite flexural strengths seemed unaffected after immersion in water for 24 h (Fig. 6) despite large differences in the amount of water uptake (Fig. 5). The addition of MAPP into unmodified-WF/PP composites sharply improved the composite flexural strengths (composites 1–4). But when C_8-WF(DMF) was used in the composite, the flexural strength was only about 53% of that of the unmodified-WF/PP composite (composite 5 versus composite 1). Using the C_8-WF(CHCl$_3$) as the reinforcing fiber decreased the flexural strength by about 10% (Fig. 6, composite 6 versus 1).

The addition of 1% MAPP into unmodified-WF/PP (60/100) composites did not increase the composite modulus (composite 2 in Fig. 7). But the addition of both 2% and 5% MAPP did significantly increase the moduli (composites 3 and 4). The flexural moduli steadily increased as the amount of MAPP was raised from 1% to 5%. C_8-WF(DMF)/PP (60/100) and C_8-WF(CHCl$_3$)/PP (60/100) composites had sharply lower flexural moduli than unmodified-WF/PP and unmodified-WF/MAPP/PP composites (composites 5 and 6 versus composites 1–4 in Fig. 7). As observed with flexural strengths, the C_8-WF(DMF)/PP composite had, by far, the lowest moduli in the series. Their moduli were only ~36% of the corresponding value for the unmodified-WF/PP (60/100) analogs.

The flexural moduli for the unmodified-WF/PP (60/100) composites decreased ~400 MPa (~18%) after 24-h water immersion. The moduli of the unmodified-WF/MAPP/PP composites also dropped but by small amounts after the 24-h water immersion (composites 1–4 in Fig. 7). Finally, the C_8-WF(DMF)/PP (60/100) and C_8-WF(CHCl$_3$)/PP (60/100) composites did not show any significant changes in flexural moduli after 24 h of water immersion (composites 5 and 6).

It is well known that small molecules can be grafted to surface sites in higher surface densities than polymeric molecules using the "grafting to" approach. As polymers react at a surface, they create diffusion barriers to the approach of other polymeric reagents to the surface [16, 17]. This is why the creation of dense polymeric brushes on surfaces must be made by growing the surface-bound polymer chains from densely grouped initiation sites [18]. Therefore, the fraction of hydroxyl groups in the WF's surface region esterified by excess octanoyl chloride is far higher than that which reacts with MAPP.

The small size of octanoyl chloride does not block further esterifications at nearby hydroxyl functions. Conversely, large MAPP molecules react with only a small fraction of surface hydroxyl functions because the diffusion of these large molecules (MW: 47000) to the region of the surface already reacted with one MAPP is blocked. Thus, the surface hydrophobicity becomes greater after WF is esterified by octanoyl chloride. This hydrophobicity should increase compatibility with PP (Van der Waals forces, dispersion forces). However, the alkyl chain of an octanoyl ester is not long enough to form effective entanglements with PP at the matrix/fiber interface. As a strain occurs under an applied stress, octanoyl chains and PP molecules which might have some small loop-like interactions, can disentangle at rates far faster than that at which strain occurs. Therefore, entanglements cannot contribute to adhesion to improve the composite flexural properties. However, the long polymer chains of MAPP can form entanglements with the PP matrix that require significant times to unravel during strain development, and so the addition of MAPP improves the unmodified-WF/PP composite flexural properties. Further support for this finding is provided in the section "SEM of Modified WF/PP Composite Fracture Surfaces".

When C_8-WF was shaken vigorously in hexane, C_8-WF dispersed well but when shaken in water, the C_8-WF agglomerated and floated on the surface. Therefore, both dispersion and Van der Waals forces must be enhanced between WF and PP after C_8-modification. Obviously, C_8-WF is more readily wetted by PP than unmodified WF is and unmodified WF is wetted well by water. How, then, could the composite flexural moduli be decreased upon replacing unmodified-WF/PP (60/100) with C_8-WF(CHCl$_3$)/PP (60/100)? This phenomenon is not understood. A few hypotheses are now suggested.

First, the C_8-modification process may affect the surface roughness at a scale not obviously visible by SEM examinations. This may reduce some WF/PP interlocking or allow some sliding motion to occur more readily at the interface. C_8-modification may change the mechanical properties of outer 500-nm thick surface region of WF.

This may tend to fail or result in a lower adhesive shear resistance. The C_8-chains are chemically bound to WF surfaces by ester bonds and the WF was carefully washed after esterification. Therefore, release of octanoic acid into the PP to serve as some sort of plasticizer can be definitely ruled out. Another possibility is that the esterification procedure may have changed the overall mechanical properties of WF in some way. This is easily imagined for the C_8-DMF treatment, where DMF solvation and extensive internal esterification may have changed the fiber properties. This explanation seems less likely for the milder, more surface-specific, C_8-$CHCl_3$ treatment. Nevertheless, it is possible that removal of some extractives by $CHCl_3$ during esterification has changed the WF fiber properties in some manner. Such changes, in turn, could decrease the flexural moduli. The C_8-WF(DMF)/PP system (with significant internal esterification) is, by far, the most seriously impacted system (Figs. 6 and 7).

SEM of modified WF/PP composite fracture surfaces

SEM micrographs of the fracture surfaces of C_8-WF ($CHCl_3$)/PP (60/100) composites illustrate that the modified WF was well dispersed in the composites (Fig. 8a, b). Some protruding WFs were found on the fracture surfaces (Fig. 8a, b). The C_8-WF($CHCl_3$) was covered with what looks like a waxy layer and it was not visibly bonded to the PP matrix (Fig. 8c). Voids existed between the C_8-WF ($CHCl_3$) and PP matrix (Fig. 8d). The C_8-WF($CHCl_3$)/PP absorbed substantially less water after immersion than unmodified-WF/PP (60/100) composite despite the poor bonding observed between C_8-WF and PP matrix. Despite absorbing much less water, the poor C_8-WF($CHCl_3$)–PP adhesion leads to lower flexural moduli and strengths compared with those of the corresponding unmodified-WF/PP composites. C_8-WF(DMF)/PP (60/100) composites also exhibited the same poor WF adhesion to PP (Fig. 9), and substantial losses in flexural strength and modulus. The alkyl chains of the grafted ester groups do not effectively entangle with the PP matrix, so the adhesion between C_8-WF and PP is poor. This reduced adhesion may allow some separation (voids) between the WF and PP to occur due to contraction on cooling after hot pressing. However, no suitable techniques to probe this possibility were available.

Figure 10 illustrates unmodified-WF/MAPP/PP (60/5/100) composite fracture surfaces. These exhibit good WF–PP adhesion. Very few WF fibers were observed at these fracture surfaces (Fig. 10a, b). Instead, PP covers the WF surfaces. This shows that failure mainly occurred within the PP matrix instead of at the WF/matrix interfaces. Large voids were not observed at the WF to PP interface with the MAPP/PP matrix (Fig. 10c, d). The adhesion between the WF and MAPP/PP matrix was good. When

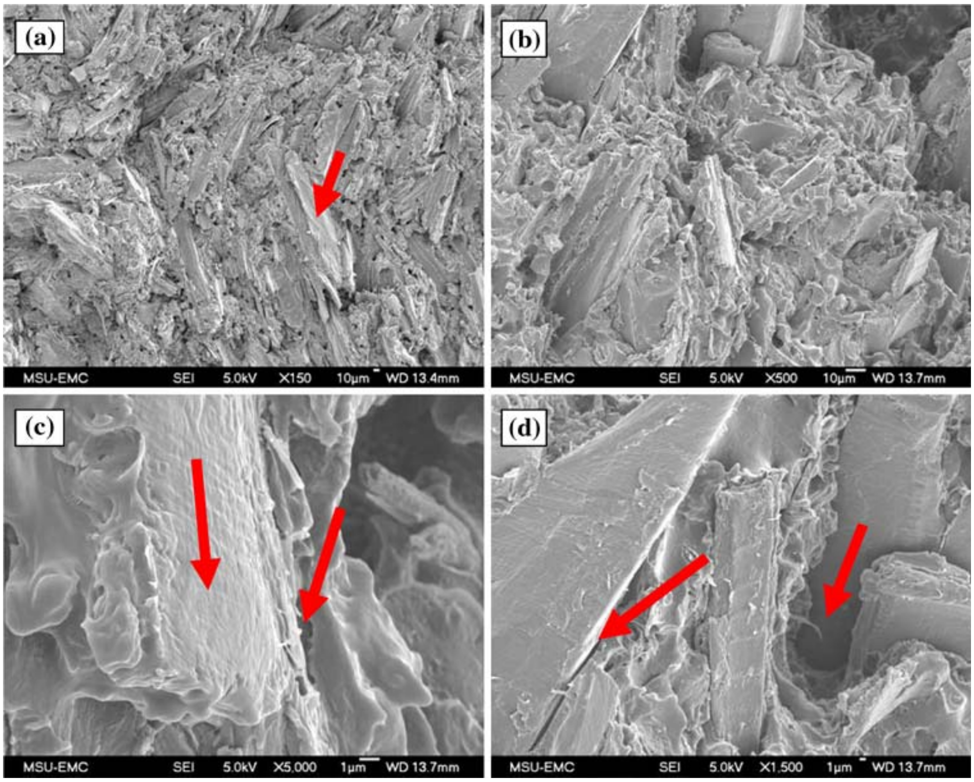

Fig. 8 SEM fracture surface micrographs of C_8-WF($CHCl_3$)/PP (60/100) composites. **a**, **b** Overall C_8-WF($CHCl_3$) dispersion; **c** poor bonding and voids between the C_8-WF($CHCl_3$) surface waxy layer and PP matrix; **d** voids between C_8-WF($CHCl_3$) and PP matrix

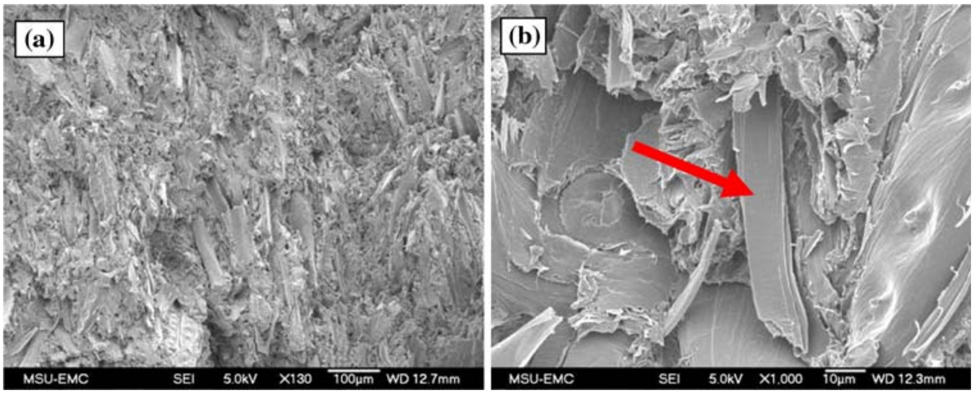

Fig. 9 SEM fracture surface micrographs of C_8-WF(DMF)/PP (60/100) composites. **a** Overall C_8-WF(DMF) dispersion; **b** poor bonding between the C_8-WF(DMF) and PP matrix (see *arrow*)

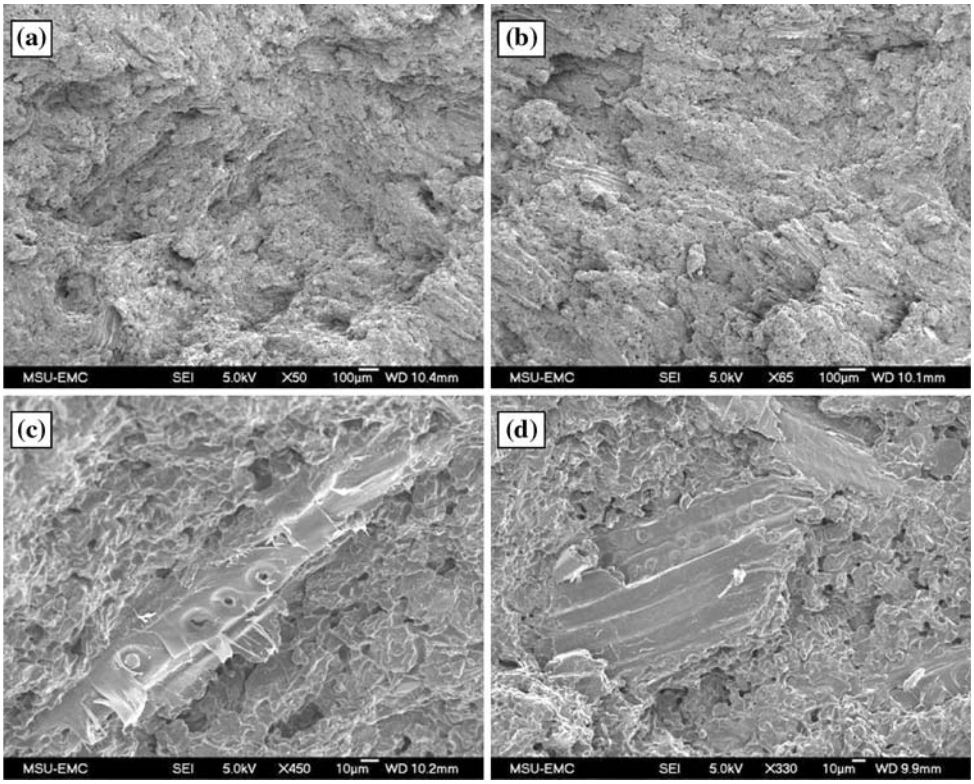

Fig. 10 SEM fracture surface micrographs of unmodified-WF/MAPP/PP (60/5/100) composites. **a**, **b** Overall WF dispersion; **c**, **d** good bonding between WF and MAPP/PP matrix

MAPP is added to the PP matrix, the anhydride groups of MAPP react with the unmodified-WF surface –OH groups during the hot (182 °C) melt extrusion processing. The long MAPP chains, attached to the WF, entangle with the PP matrix. These factors contribute to the excellent unmodified-WF–MAPP/PP adhesion and mechanical property improvements that this causes.

Conclusions

The properties of unmodified-WF/PP composites were largely dependent on the unmodified-WF content. Higher unmodified-WF content led to higher composite stiffness, higher water uptake, but lower flexural strength. The flexural moduli of unmodified-WF/PP composites decreased after 24 h of water immersion, but the flexural strengths were little affected.

Modification of WF by octanoyl chloride esterification greatly reduced C_8-WF/PP composite water absorption, but it also decreased both the composites' flexural strengths and flexural moduli. C_8-modified WF exhibited poorer adhesion to PP matrix under stress than unmodified-WF (SEM) despite the better match in surface energies between C_8-WF and PP (both hydrophobic). MAPP, in contrast, improved unmodified-WF–PP adhesion. Addition of MAPP to WF/PP composites improved composite flexural strengths, flexural moduli, and water uptake resistance. Higher MAPP loadings (between 1% and 5%) favor progressively better composite flexural properties.

MAPP enhances mechanical properties mainly by forming MAPP/PP entanglements at the WF surfaces. These entanglements allow better stress transfer between the polymer and fiber. Modification of WF surfaces with C_8 ester groups lowers the rate of water uptake and enhances surface hydrophobicity. However, making the surface hydrophobic by this treatment did not improve mechanical properties. Apparently, entanglements are the major enhancers of the mechanical properties. Kazayawoko et al. [19] demonstrated that MAPP improved the tensile strength of wood veneer/PP and wood fiber/PP composites and attributed these improvements to the reduction of wood fiber surface energy, improved fiber dispersion, improved fiber orientation, and enhanced interfacial adhesion through mechanical interlocking. They mentioned interchain entanglements between PP and surface-bound MAPP but did not further emphasize it. In our study, the octanoyl chloride-esterified WF has a low surface energy, similar to MAPP-esterified WF. So surface activity in both cases will lead to PP/WF-surface compatibility. Our process does not orient the fibers; so, no fiber orientation effects can explain the differences in mechanical properties given by MAPP-modification versus C_8-modification. Our observations are consistent with no differences in fiber dispersion between these two systems. Thus, mechanical interlocking, based on the net geometry of fiber surface shape surrounded by polymers, cannot explain the differences. Thus, we conclude that entanglements between surface-bound MAPP and matrix PP must play a major role in the mechanical property differences for the WF/PP composites prepared in this article.

Acknowledgements This work was funded by Center for Advanced Vehicular Systems of Mississippi State University ("Hybrid composites for a hybrid car" project). This work was also partly supported by the Forest Products Laboratory at Mississippi State University. The SEM characterization was supported by MCL Follow-up Funding from Mississippi State University. The authors thank Mr. Dustin Black for performing water absorption and third-point bending measurements. The authors also thank Ms. Amanda M. Lawrence for her help in SEM characterization.

References

1. Clemons CM (2000) Proceedings of the 3rd international wood and natural fibre composites symposium, Kassel, Germany
2. Magurno A (1999) Die Angewandte Makromolekulare Chemie 272(1):99
3. Bledzki AK, Faruk O, Sperber VE (2006) Macromol Mater Eng 291(5):449. doi:10.1002/mame.200600113
4. Tshabalala MA, Kingshott P, Vanlandingham MR, Plackett D (2003) J Appl Polym Sci 88:2828. doi:10.1002/app.12142
5. Tserki V, Matzinos P, Kokkou S, Panayiotou C (2005) Compos, Part A 36:965. doi:10.1016/j.compositesa.2004.11.010
6. Zhang C, Li KC, Simonsen J (2004) J Adhes Sci Technol 18:1603
7. Ellis WD, O'Dell JL (1999) J Appl Polym Sci 73:2493
8. Sèbe G, Tingaut P, Safoutchiama R, Pétraud M, Grelier S, Jéso BD (2004) Holzforschung 58:511. doi:10.1515/HF.2004.078
9. Oksman K, Clemons C (1998) J Appl Polym Sci 67(9):1503
10. Cantero G, Arbelaiz A, Mugika F, Valea A, Mondragon I (2003) J Reinf Plast Compos 22(1):37. doi:10.1177/0731684403022001495
11. Kaci M, Cimmino S, Silvestre C, Duraccio D, Benhamida A, Zaidi L (2006) Macromol Mater Eng 291(7):869. doi:10.1002/mame.200600003
12. Wu JS, Yu DM, Chan CM, Kim J, Mai YW (2000) J Appl Polym Sci 76:1000
13. Zhang Y, Pittman CU Jr, Toghiani H, Zhang J, Xue Y (2009) Compos Interfaces (accepted)
14. ASTM D 790-92
15. ASTM D 570-98
16. Wu Z, Pittman CU Jr, Gardner SD (1996) Carbon 34(1):59. doi:10.1016/0008-6223(95)00135-2
17. Tsubokawa N, Kobayashi K, Sone Y (1988) J Polym Sci, Part A: Polym Chem 26:223. doi:10.1002/pola.1988.080260122
18. Edmondson S, Osborne VL, Huck WTS (2004) Chem Soc Rev 33:14. doi:10.1039/b210143m
19. Kazayawoko M, Balatinecz JJ, Matuana LM (1999) J Mater Sci 34:6189. doi:10.1023/A:1004790409158